RSC Advances

PAPER

View Article Online
View Journal | View Issue

Cite this: *RSC Adv.*, 2017, **7**, 40615

A highly selective ratiometric fluorescent probe for the cascade detection of Zn^{2+} and $H_2PO_4^-$ and its application in living cell imaging†

Kui Du,[ab] Shizhen Niu,[a] Li Qiao,[b] Yandong Dou,[c] Qing Zhu,[c] Xinzhi Chen*[a] and Pengfei Zhang*[b]

Received 20th July 2017
Accepted 12th August 2017

DOI: 10.1039/c7ra08020d

rsc.li/rsc-advances

A simple ratiometric sensor (L_1) for the cascade detection of Zn^{2+} and $H_2PO_4^-$ with high selectivity was reported based on the intermolecular charge transfer (ICT) mechanism. This new sensor could distinguish Zn^{2+} from Cd^{2+}, and features high fluorescence quantum yield with L_1 (0.45) and L_1–Zn^{2+} (0.27). There is a good linear relationship between the fluorescence ratio $I_{525\ nm}/I_{430\ nm}$ upon addition of Zn^{2+} and the limit of detection (LOD) was evaluated to be 41.0 nM. Furthermore, the *in situ* prepared L_1–Zn^{2+} complex also displayed good selectivity and ratiometric response for $H_2PO_4^-$ and the detection limit of L_1–Zn^{2+} was found to be 49.0 nM. L_1 exhibits permeability and can been applied to the detection of intracellular Zn^{2+} and $H_2PO_4^-$ in HepG-2 cells.

Introduction

Zinc plays important roles in gene transcription, cellular metabolism, immune function, and so on.[1] It is also involved in neurological disorders such as Alzheimer's disease, ischemic stroke, cerebral ischemia and infantile diarrhea.[2] Therefore, unravelling the processes in facilitating essential biological functions of mobile zinc ions in living cells is of significant interest.[3] On the other hand, a simple and rapid method for determination of dihydrogen phosphate ($H_2PO_4^-$), which is the predominant equilibrium species of inorganic phosphate at physiological pH, is still in high demand.[4]

Fluorescent chemosensors have played an important role in the recognition of biologically important species, such as metal ions and anions, due to the simplicity and high sensitivity of fluorescence assays.[5] The receptor, which is referred to as the central processing unit (CPU) of a chemosensor, plays a significant role in the designing of new fluorescent chemosensors, especially for the quinoline-based receptor.[6] In recent years, numerous chemosensors with good recognition sites for a single species have been developed. However, fluorogenic receptors for the fluorescent chemosensors that allow the cascaded detection of multiple analytes with high selectivity are still desirable.[7] Although, several fluorescent chemosensors with good recognition site has been designed for both zinc and dihydrogen phosphate,[8] the ratiometric fluorescent probe with excellent selectivity for the cascade detection of the Zn^{2+} and $H_2PO_4^-$ is still a big challenge.[9]

Our research group involves the design and synthesis of novel 8-aminoquinoline derivatives and its application in the biological fields.[10] In continue our work, herein; we have reported a novel receptor for the cascade detection of Zn^{2+} and $H_2PO_4^-$ with high selectivity through introducing of the tetrahydrofuran on to the carboxamidoquinoline. Furthermore, based on the intermolecular charge transfer (ICT) mechanism,[11] a new fluorescent chemosensors L_1 was designed with excellent ratiometric fluorescence response for the detection of Zn^{2+} ions and $H_2PO_4^-$. And this new sensor has displayed a good application prospect in cell image.

Results and discussion

Synthesis

The synthesis of the L_1 was described in Scheme 1. L_1 was synthesized in two steps. Starting from compound **1**, compound

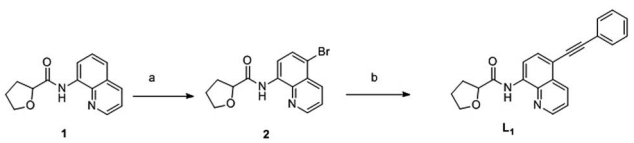

Scheme 1 The facile synthesis of L_1. Reagents, conditions and yields: (a) $Cu(OAc)_2$, $PhI(OAc)_2$, PivOH, NaBr, 1,4-dioxane, air, 50 °C, 15 min, 87%; (b) phenylacetylen, $PdCl_2(PPh_3)_2$, Et_3N, DMF, 60 °C, 24 h, 72%.

[a]*Key Laboratory of Biomass Chemical Engineering of Ministry of Education, College of Chemical and Biological Engineering, Zhejiang University, Hangzhou, 310027, P. R. China. E-mail: 15268560133@163.com*

[b]*College of Material Chemistry and Chemical Engineering, Hangzhou Normal University, Hangzhou, 310036, P. R. China*

[c]*Key Laboratory of Bioorganic Synthesis of Zhejiang Province, College of Biotechnology and Bioengineering, Hangzhou 310014, China*

† Electronic supplementary information (ESI) available. See DOI: 10.1039/c7ra08020d

2 was achieved in the presence of NaBr, $PhI(OAc)_2$ and PivOH with $Cu(OAc)_2$ as the catalyst. Then compound **2**, phenylacetylene, $PdCl_2(PPh_3)_2$ and Et_3N were added in DMF and reacted at 60 °C for 24 h, the target product $\mathbf{L_1}$ was obtained.

Fluorescence response for Zn^{2+}

We implemented the spectroscopic properties of $\mathbf{L_1}$ for Zn^{2+} using the UV-Vis and fluorescence spectroscopy studies in DMSO/H_2O (8 : 2, v/v). The absorption spectrum of $\mathbf{L_1}$ exhibited two absorption bands at 280 nm and 360 nm corresponding to phenylene-ethynylene.[12] Upon addition of Zn^{2+} ions (0–8 equiv.) to the solution of $\mathbf{L_1}$, resulted in the red shift of the absorption band center at 360 nm to 420 nm, along with the formation of a clear isosbestic point at 385 nm, indicating formation of $\mathbf{L_1}$–Zn^{2+} complex (Fig. S1†).

In order to evaluate the selectivity of $\mathbf{L_1}$ for Zn^{2+}, the fluorescence changes of $\mathbf{L_1}$ to various metal ions (Mg^{2+}, Na^+, Cu^{2+}, Hg^{2+}, K^+, Al^{3+}, Fe^{3+}, Ca^{2+}, Ag^+, Ba^{2+}, Co^{2+}, Pb^{2+}, Mn^{2+}, Ni^{2+}, Cr^{3+}, Zn^{2+} and Cd^{2+}) were investigated in DMSO/H_2O (8 : 2, v/v). Sensor $\mathbf{L_1}$, upon excitation at 390 nm, displayed a strong emission band centered at 430 nm which contribute to the introducing of the phenylene-ethynylene. Upon addition of 12 equiv. Zn^{2+} ion, the emission band at 430 nm decreased dramatically, meanwhile, a new emission band centered at 525 nm with a remarkable red-shift of 95 nm were observed (Fig. 1a). It can be attributed to an ICT process in the excited state of $\mathbf{L_1}$–Zn^{2+}.[13] In this situation, electron transfer from amide nitrogen adjacent to the quinoline which was substituted with phenylene-ethynylene at C-5 position to Zn^{2+} enhanced the ICT process of $\mathbf{L_1}$, and an obviously red-shift of 95 nm was achieved. Simultaneously, an apparently yellow emission of the solution can be visualized through the naked eye under a UV lamp (365 nm, Fig. 1b). While addition of other metal cations, no significant spectral changes were observed except Cu^{2+} and Hg^{2+}, which shown fluorescence quenching effects. These results indicated that $\mathbf{L_1}$ can readily recognize Zn^{2+} from other ions through the obviously red-shift fluorescence. Furthermore, a competition experiment was conducted through adding Zn^{2+} (12 equiv.) to $\mathbf{L_1}$ solution in the presence of other metal ions (12 equiv.), which demonstrated that no obvious interference was observed except for Cu^{2+} and Hg^{2+} (Fig. 2).

In an attempt to evaluate the sensing property of sensor $\mathbf{L_1}$ to Zn^{2+}, fluorescence titration experiments were conducted. As shown in Fig. 3, the emission intensity at 430 nm was gradually decreased, while a new emission band appeared at 525 nm with gradual increasing upon addition of Zn^{2+} ions. And the well-defined isoemissive point was observed at 475 nm. The fluorescence quantum yield of the $\mathbf{L_1}$–Zn^{2+} complex was calculated to be 0.27 (at 525 nm) as compared to that of free $\mathbf{L_1}$ (0.45 at

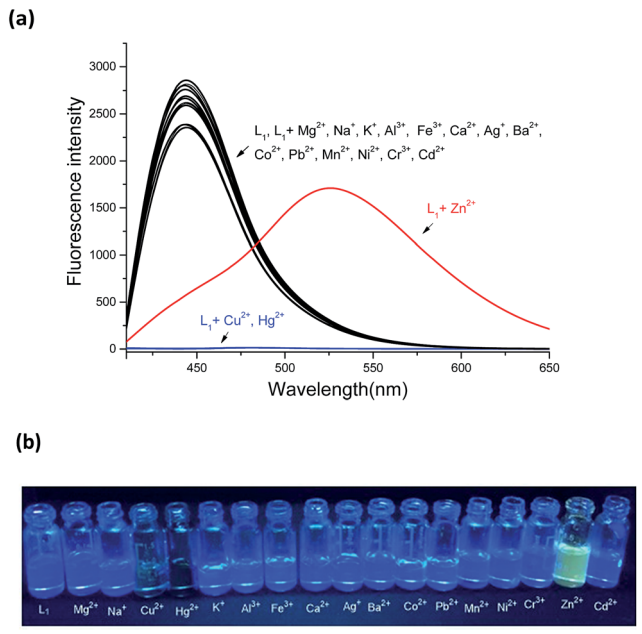

Fig. 1 (a) Fluorescence (λ_{ex} = 390 nm) responses of $\mathbf{L_1}$ (5 μM) upon addition of various metal ions (60 μM) in DMSO/water (v/v = 8/2); (b) visual changes in fluorescence of $\mathbf{L_1}$ in the presence of metal ions.

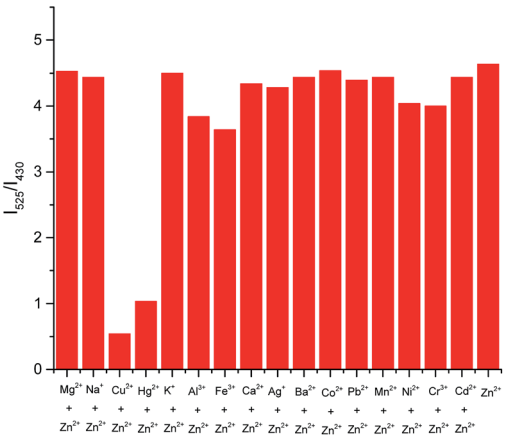

Fig. 2 The ratio fluorescence responses ($I_{525\ nm}/I_{430\ nm}$) of $\mathbf{L_1}$ (5 μM) containing 60 μM Zn^{2+} to the selected metal ions: 12 equiv. of Mg^{2+}, Na^+, Cu^{2+}, Hg^{2+}, K^+, Al^{3+}, Fe^{3+}, Ca^{2+}, Ag^+, Ba^{2+}, Co^{2+}, Pb^{2+}, Mn^{2+}, Ni^{2+}, Cr^{3+}, Cd^{2+} in DMSO/water (v/v = 8/2).

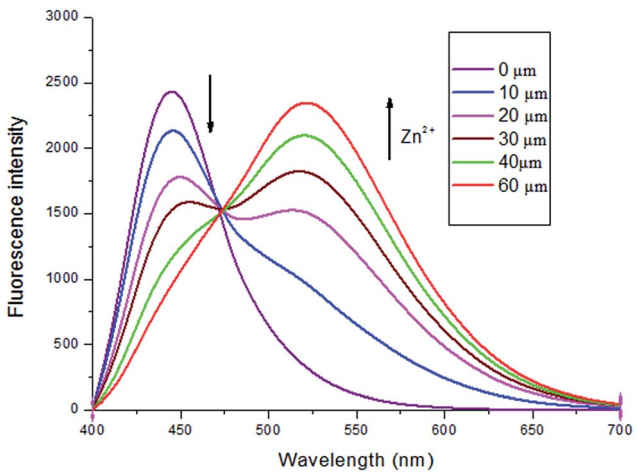

Fig. 3 Fluorescence spectra of $\mathbf{L_1}$ (5 μM) in the presence of different concentration of Zn^{2+} in DMSO/H_2O (v/v = 8 : 2), λ_{ex} = 390 nm.

430 nm). This ratiometric fluorescence behavior of $\mathbf{L_1}$ with Zn^{2+} ions is attributed to internal charge transfer (ICT) mechanisms. From the titration profile, the binding constant of $\mathbf{L_1}$ and Zn^{2+} was evaluated to be $1.94 \times 10^4\ M^{-1}$ (Fig. S2†).[7a,d] The detection limit of $\mathbf{L_1}$ for Zn^{2+} ions was determined to be 41.0 nM which is sufficiently low for the detection of Zn^{2+} ions in intracellular and *in vivo*[11d] (Fig. S3†).

For better understanding the interaction of $\mathbf{L_1}$ with Zn^{2+}, ^1H NMR spectra of $\mathbf{L_1}$ in the absence and presence of Zn^{2+} (12.0 equiv.) were conducted (Fig. 4). On complexation of $\mathbf{L_1}$ with Zn^{2+}, amide proton was diminished, ascribed to the interaction between metal and carboxamido group.[14] And all protons of the quinoline or tetrahydrofuran moieties changed accordingly, demonstrated that the direct interaction between the ligating groups of the probe and Zn^{2+}. Moreover, the release of $\mathbf{L_1}$ when added $H_2PO_4^-$ to the $\mathbf{L_1}$–Zn^{2+} solution was displayed through the ESI-Mass spectra, in which two peaks at *m*/*z* 343.1444 assigned to $[\mathbf{L_1} + H^+]$ and at *m*/*z* 406.2726 assigned to $[\mathbf{L_1} + Zn^{2+} + H^+]$ were observed (Fig. S4†). The Job's plot analysis indicated that 1 : 1 binding stoichiometry between $\mathbf{L_1}$ and Zn^{2+} (Fig. 5). And the proposed mechanism of $\mathbf{L_1}$ for the cascade detection of Zn^{2+} and $H_2PO_4^-$ was displayed in Fig. S5.†

Subsequently effects of pH on the fluorescence of $\mathbf{L_1}$ with Zn^{2+} also were investigated. As shown in Fig. 6, $\mathbf{L_1}$ displayed weak fluorescence response to Zn^{2+} in an acidic environment

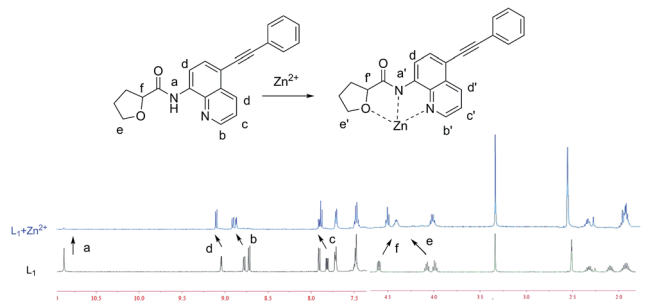

Fig. 4 ^1H NMR spectrum of L_1 (DMSO-d_6) in the absence and presence of Zn^{2+}.

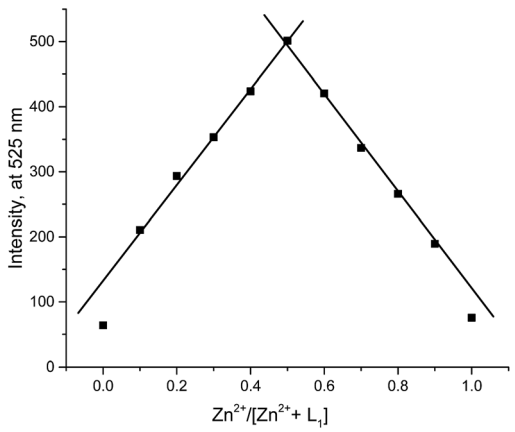

Fig. 5 Job's plot for L_1–Zn^{2+} complex in DMSO/H_2O (v/v = 8 : 2). The total concentration of Zn^{2+} and L_1 is 10 μM. λ_{ex} = 390 nm.

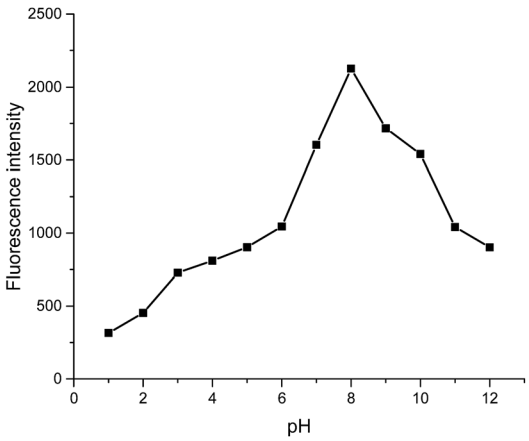

Fig. 6 Effect of pH on the fluorescence intensity of L_1 (5 μM) with Zn^{2+} (12 equiv.) in DMSO/water (v/v, 8/2) (λ_{ex} = 390 nm, λ_{em} = 525 nm).

(pH < 5) contribute to the protonation of the amino group in $\mathbf{L_1}$, resulted in weak coordination ability to Zn^{2+}. However, the Zn^{2+} detection abilities of $\mathbf{L_1}$ can be achieved when the pH increased from 6 to 11. At pH 7.5, the fluorescence intensity reached its optimum point at 525 nm, indicating that $\mathbf{L_1}$ possess the highest sensing ability under the physiological pH window. Therefore, all the fluorescence detection processes were performed at pH 7.5.

Fluorescence sensing of L_1–Zn^{2+} complex for $H_2PO_4^-$

Then $\mathbf{L_1}$–Zn^{2+} complex were further conducted as a secondary sensor system towards $H_2PO_4^-$ recognition *via* the relay recognition approach. To evaluate the selective detection of $H_2PO_4^-$ with various anions, F^-, Cl^-, Br^-, AcO^-, PO_4^{3-}, PPi, CO_3^{2-}, HSO_4^-, CN^- and SO_4^{2-} (14 equiv.) were added to the solution of the $\mathbf{L_1}$–Zn^{2+} complex. As shown in Fig. 7, the addition of $H_2PO_4^-$ (14 equiv.) to the solution of $\mathbf{L_1}$–Zn^{2+} complex resulted in the appearance of fluorescence emission at 430 nm along with

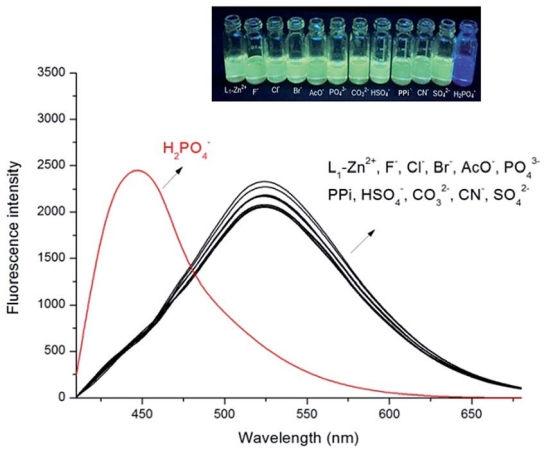

Fig. 7 Fluorescence spectra of L_1 (5 μM) upon addition of various anions to the L_1–Zn^{2+} complex in DMSO/H_2O (v/v = 8 : 2); the inset shows visual changes in fluorescence of L_1–Zn^{2+} in the presence of anions.

simultaneous decease at 525 nm. And the solution turned to the original blue color from yellow (Fig. 7). The revival of probe $\mathbf{L_1}$ fluorescence at 430 nm is contributed to the coordination of $H_2PO_4^-$ with Zn^{2+}. However, the addition of other inorganic anions such F^-, Cl^-, Br^-, AcO^-, PO_4^{3-}, PPi, CO_3^{2-}, HSO_4^-, CN^- and SO_4^{2-} (14 equiv.) did not show any obvious changes in fluorescence response (Fig. S6†).

The fluorescence titration experiments also were conducted to estimate the sensing property of sensor $\mathbf{L_1}$–Zn^{2+} to $H_2PO_4^-$ (Fig. 8). The emission intensity at 430 nm was gradually increased, while emission intensity at 525 nm with gradual decreasing upon addition of $H_2PO_4^-$ ions. Addition of 14 equiv. $H_2PO_4^-$ (70 μM) to the solution resulted in absolutely quenching of the fluorescence emission of the $\mathbf{L_1}$–Zn^{2+} complex. Furthermore, the $\mathbf{L_1}$–Zn^{2+} complex provided an excellent ratiometric system for the detection of $H_2PO_4^-$ in DMSO/H_2O (8 : 2, v/v). And the detection limit of $\mathbf{L_1}$–Zn^{2+} for $H_2PO_4^-$ ions was determined to be 49.0 nM [Fig. S7†].

Application of fluorescence detection of Zn^{2+} and $H_2PO_4^-$ ions in living cells

To further assess fluorescence detection of Zn^{2+} and $H_2PO_4^-$ ions in biological samples, fluorescent imaging inside HepG-2 cells were performed by the bio-imaging process. Firstly, the cytotoxicity which plays the important factor in live cell imaging of the $\mathbf{L_1}$ was assessed by MTS assays in HepG-2 cells (Fig. S8†). The result indicating that low micromolar concentrations of $\mathbf{L_1}$ were almost free of toxicity to the HepG-2 cells. Although treatment with 50 μM of $\mathbf{L_1}$ at 24 h, the cell survival decreased, no significant loss of cells were noticed, suggesting that this new sensor can be applied in the cell imaging.

Incubation of HepG-2 cells with 5 μM of $\mathbf{L_1}$ in TBS buffer before imaging for 30 min at 37 °C showed in the blue channel which indicated the emissive nature of $\mathbf{L_1}$ in the intracellular system (Fig. 9a–c). While, the addition of Zn^{2+} (40 μM) to cells with receptor $\mathbf{L_1}$ (5 μM) showed fluorescence emission in the yellow channel (Fig. 9d–f). These results suggest that $\mathbf{L_1}$ is cell permeable and can be further designed as a biomaterial for the probing of bioactive analytes in the cellular environment with the change in fluorescence emission from blue to yellow. Moreover, the successive interaction of $H_2PO_4^-$ (60 μM) towards the $\mathbf{L_1}$–Zn^{2+} complex was conducted. The yellow fluorescence turned off upon the addition of NaH_2PO_4, along with the fluorescence revival of probe $\mathbf{L_1}$ (Fig. 9g–i). Hence, $\mathbf{L_1}$ has potential applicability for detecting Zn^{2+} and $H_2PO_4^-$ in biological samples *via* the relay recognition approach.

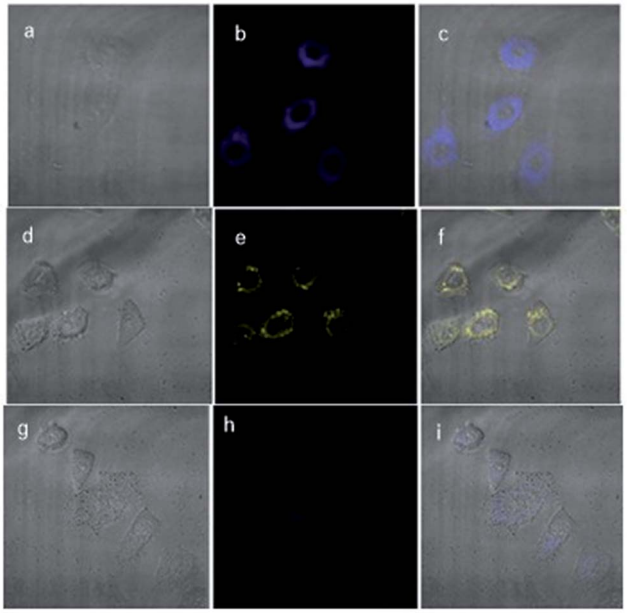

Fig. 9 Fluorescence and bright field images of HepG-2 cell lines. Image (b) is the fluorescence image of cells in the blue channel treated with probe $\mathbf{L_1}$ (5 μM) for 30 min at 37 °C; (a) is the bright field image of (b); image (c) is the overlay of (b) and (a). Image (e) is the fluorescence image of cells in the yellow channel upon treatment with $\mathbf{L_1}$ (5 μM) and then Zn^{2+} (40 μM) for 30 min at 37 °C; (d) is the bright field image of (e); image (f) is the overlay of (d) and (e). Image (h) is the fluorescence image of cells in the blue channel upon treatment with $\mathbf{L_1}$ (5 μM), Zn^{2+} (40 μM) and then $H_2PO_4^-$ (60 μM) for 30 min at 37 °C; (g) is the bright field image of (h); image (i) is the overlay of (g) and (h); λ_{ex} = 400 nm.

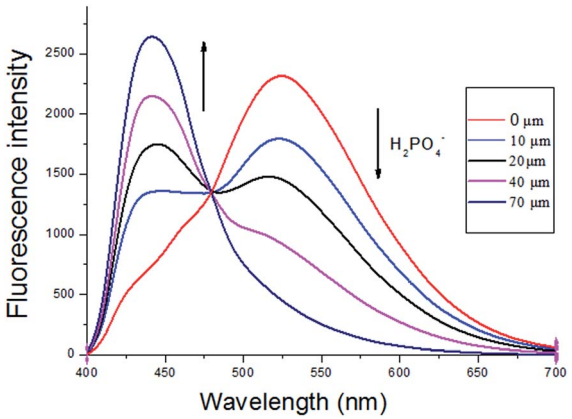

Fig. 8 Fluorescence spectra of $\mathbf{L_1}$–Zn^{2+} (5 μM) in the presence of different concentration of $H_2PO_4^-$ in DMSO/H_2O (v/v = 8 : 2), λ_{ex} = 390 nm.

Conclusions

In summary, we have developed a novel fluorescent $\mathbf{L_1}$ with tetrahydrofuran-2-carboxamidoquinoline as the new receptor. Sensor $\mathbf{L_1}$ displayed highly selective and ratiometric fluorescence responses to Zn^{2+} at physiological pH condition. Moreover, the *in situ* formed $\mathbf{L_1}$–Zn^{2+} complex demonstrated reversible, selective and good ratiometric response for the $H_2PO_4^-$. The detection limit of $\mathbf{L_1}$ to Zn^{2+} and $\mathbf{L_1}$–Zn^{2+} complex to $H_2PO_4^-$ was found to be 41.0 nM and 49.0 nM respectively. Furthermore, the intracellular detection of Zn^{2+} ions by $\mathbf{L_1}$ and $H_2PO_4^-$ ions by the $\mathbf{L_1}$–Zn^{2+} complex was also conducted in the HepG-2 cell lines. These results suggest that $\mathbf{L_1}$ and the *in situ* formed $\mathbf{L_1}$–Zn^{2+} complex are cell permeable and can be further designed as a biomaterial for the probing of bioactive analytes in the cellular environment with the change in fluorescence emission between blue to yellow.

Experimental section

Materials and general methods

The reagents and solvents for the present study were purchased from commercial suppliers and used as received. Absorption measurements were carried out using a JASCO-V630 spectrophotometer. Fluorescence spectra were recorded on SpectraMax M5. ^{1}H NMR and ^{13}C NMR spectra were recorded using a Bruker DRX-500 spectrometer. All of the chemical shifts were reported in ppm and coupling constants (J) in hertz. High-resolution mass spectroscopy (HRMS) was measured on a Bruker micrOTOF-Q mass spectrometer (BrukerDaltonik, Bremen, Germany). The pH measurements were made using a Mettler Toledo FE20 pH meter. Fluorescence imaging experiments were performed using a Zeiss Axiovert 200M inverted epifluorescence microscope with a Hamamatsu EM-CCD digital camera C9100 and a MS200 XY Piezo Z stage (Applied Scientific Instruments, Inc.). The cytotoxicity of $\mathbf{L_1}$ was evaluated by the MTS assay (BB-4204-250T).

Cell imaging experiments

The HepG-2 cells were cultured in Dulbecco's Modified Eagle Medium (DMEM, GIBCO), supplemented with 10% heat-deactivated fetal bovine serum (FBS) and 1% penicillin/streptomycin, at 37 °C in a humidified atmosphere with 5% CO_2.[15] In order to get the cell image, the HepG-2 cells were seeded in 6-well flat-bottomed plates one day before. 5 μm of $\mathbf{L_1}$ was added to the HepG-2 cells and incubated for 0.5 h at 37 °C under 5% CO_2 and the fluorescence imaging of intracellular Zn^{2+} was observed under inverted fluorescence microscope, the image last for 5 min. And then the cells were washed with TBS for three times, subsequently incubating with 40 μm Zn^{2+} for another 0.5 h, then the image was achieved. After rinsed with TBS for another three times of the cells, NaH_2PO_4 solutions (60 μm) were added in the cells. The imaging was started immediately upon NaH_2PO_4 solution addition.

Synthesis

The synthesis of the $\mathbf{L_1}$ was described in Scheme 1. Compound **1** and **2** were achieved according to our previous work.[10b] The mixture of compound **2** (0.64 g, 2.0 mmol), phenylacetylene (0.25 g, 2.5 mmol), $PdCl_2(PPh_3)_2$ (15.8 mg, 0.2 mmol), Et_3N (0.40 g, 4.0 mmol), and DMF (15 mL) was heated at 60 °C for 24 h. After completion of the reaction, the mixture was filtered to remove salts and the precipitate was washed with 100 mL of ethyl acetate, and then the organic phase was added into 100 mL of water. 100 mL of ethyl acetate was used to extract the crude product from the mixture. The organic phase was removed under reduced pressure to obtain the crude product, which was purified by silica gel column with a mixture solvent of petroleum ether/ethyl acetate as the eluent.

$\mathbf{L_1}$. Yield: (615.6 mg, 90%). Mp: 119–120 °C. ^{1}H NMR (500 MHz, $CDCl_3$) δ 10.99 (s, 1H), 8.90 (dd, J = 4.2, 1.6 Hz, 1H), 8.79 (d, J = 8.1 Hz, 1H), 8.71 (dd, J = 8.4, 1.6 Hz, 1H), 7.80 (d, J = 8.1 Hz, 1H), 7.66–7.58 (m, 2H), 7.55 (dd, J = 8.4, 4.2 Hz, 1H), 7.42–7.33 (m, 3H), 4.62 (dd, J = 8.4, 5.6 Hz, 1H), 4.28–4.19 (m, 1H), 4.07 (dd, J = 15.2, 7.0 Hz, 1H), 2.45–2.38 (m, 1H), 2.27 (ddd, J = 13.0, 7.5, 6.0 Hz, 1H), 2.04–1.95 (m, 2H); ^{13}C NMR (125 MHz, $CDCl_3$) δ 171.23, 147.94, 137.56, 133.88, 133.45, 130.61, 130.56, 127.45, 127.27, 122.11, 121.16, 114.99, 114.13, 93.04, 85.35, 78.17, 68.78, 29.42, 24.55. HRMS (ESI$^+$): found $[M + H]^+$ 343.1437 $C_{22}H_{18}ClN_5O_2$ requires $[M + H]^+$ 343.1444.

Conflicts of interest

There are no conflicts to declare.

Acknowledgements

Financial support from the Natural Science Foundation of Zhejiang Province (No. LZ13B020001), the National Natural Science Foundation of China (No. 21376213, No. 21376058).

Notes and references

1 (*a*) A. I. Bush, W. H. Pettingell, G. Multhaup, M. D. Paradis, J. P. Vonsattel, J. F. Gusella, K. Beyreuther, C. L. Masters and R. E. Tanzi, *Science*, 1994, **265**, 1464; (*b*) J. M. Berg and Y. Shi, *Science*, 1996, **271**, 1081; (*c*) T. V. Halloran, *Science*, 1993, **261**, 715; (*d*) C. J. Frederickson, J. Y. Koh and A. I. Bush, *Nat. Rev. Neurosci.*, 2005, **6**, 449; (*e*) C. J. Frederickson and A. I. Bush, *BioMetals*, 2001, **14**, 353.

2 (*a*) J. Y. Koh, S. W. Suh, B. J. Gwag, Y. Y. He, C. Y. Hsu and D. W. Choi, *Science*, 1996, **272**, 1013; (*b*) D. W. Choi and J. Y. Koh, *Annu. Rev. Neurosci.*, 1998, **21**, 347; (*c*) C. F. Walker and R. E. Black, *Annu. Rev. Nutr.*, 2004, **24**, 255.

3 (*a*) C. Andreini, L. Banci, I. Bertini and A. J. Rosato, *Proteome Res.*, 2006, **5**, 196; (*b*) G. Salazar, B. Craige, R. Love, D. Kalman and V. Faundez, *J. Cell Sci.*, 2005, **118**, 1911; (*c*) K. Ponnuvel, V. Padmini and R. Sribalan, *Sens. Actuators, B*, 2016, **222**, 605; (*d*) Z. Guo, G. Kim, I. Shin and J. Yoon, *Biomaterials*, 2012, **33**, 7818; (*e*) G. Sivaramam, T. An and D. Chellappa, *Analyst*, 2012, **137**, 5881.

4 (*a*) A. E. Hargrove, S. Nieto, T. Zhang, J. L. Sessler and E. V. Anslyn, *Chem. Rev.*, 2011, **111**, 6603; (*b*) C. Bazzicalupi, A. Bencini and V. Lippolis, *Chem. Soc. Rev.*, 2010, **39**, 3709; (*c*) D. Zhang, J. R. Cochrane, A. Martinez and G. Gao, *RSC Adv.*, 2014, **4**, 29735.

5 (*a*) J. Yoon, S. K. Kim, N. J. Singh and K. S. Kim, *Chem. Soc. Rev.*, 2006, **35**, 355; (*b*) P. A. Gale, S. E. Garcia-Garrido and J. Garric, *Chem. Soc. Rev.*, 2008, **37**, 151; (*c*) M. Formica, V. Fusi, L. Giorgi and M. Micheloni, *Coord. Chem. Rev.*, 2012, **256**, 170.

6 (*a*) A. P. de Silva, H. Q. Nimal Gunaratne, T. Gunnlaugsson, A. J. M. Huxley, C. P. McCoy, J. T. Rademacher and T. E. Rice, *Chem. Rev.*, 1997, **97**, 1515; (*b*) Z. Xu, J. Yoon and D. R. Spring, Fluorescent chemosensors for Zn^{2+}, *Chem. Soc. Rev.*, 2010, **39**, 1996; (*c*) Y. Ma, F. Wang, S. Kambam and X. Chen, *Sens. Actuators, B*, 2013, **188**, 1116; (*d*) J. Qiang, C. Chang, Z. Zhu, T. Wei, W. Yu, F. Wang, J. Yin, Y. Wang, W. Zhang, J. Xie and X. Chen, *Sens. Actuators, B*, 2016, **233**, 591; (*e*) W. Yu, J. Qiang, J. Yin, S. Kambam, F. Wang, Y. Wang and X. Chen, *Org. Lett.*,

2014, **16**, 2220; (*f*) C. Chang, F. Wang, T. Wei and X. Chen, *Ind. Eng. Chem. Res.*, 2017, **56**, 8797.

7 (*a*) E. J. Song, H. Kim, I. H. Hwang, K. B. Kim, A. R. Kim, I. Noh and C. Kim, *Sens. Actuators, B*, 2014, **195**, 36; (*b*) Y. W. Choi, G. J. Park, Y. J. Na, H. Y. Jo, S. A. Lee, G. R. You and C. Kim, *Sens. Actuators, B*, 2014, **194**, 343; (*c*) E. J. Song, J. Kang, G. R. You, G. J. Park, Y. Kim, S. J. Kim, C. Kim and R. G. Harrison, *Dalton Trans.*, 2013, **42**, 15514; (*d*) L. Li, Y. Shen, Y. Zhao, L. Mu, X. Zeng, C. Redshaw and G. Wei, *Sens. Actuators, B*, 2016, **226**, 279; (*e*) A. Roy, S. Dey and P. Roy, *Sens. Actuators, B*, 2016, **237**, 628; (*f*) C. Patra, A. K. Bhanja, C. Sen, D. Ojha, D. Chattopadhyay, A. Mahapatra and C. Sinha, *RSC Adv.*, 2016, **6**, 53378.

8 (*a*) N. Sharma, S. I. Reja, V. Bhalla and M. Kumar, *Dalton Trans.*, 2015, **44**, 6062; (*b*) S. Suganya, S. Velmathi, P. Venkatesan, S. Wu and M. S. Boobalan, *Inorg. Chem. Front.*, 2015, **2**, 649; (*c*) A. Hens, *RSC Adv.*, 2015, **5**, 54352; (*d*) B. Shi, Y. Zhang, T. Wei, Q. Lin, H. Yao, P. Zhang and X. You, *Sens. Actuators, B*, 2014, **190**, 555; (*e*) S. Goswami, S. Maity, A. C. Maity, A. K. Das, K. Khanra, T. K. Mandal and N. Bhattacharyy, *Tetrahedron Lett.*, 2014, **55**, 5993; (*f*) A. Gogoi, S. Samanta and G. Das, *Sens. Actuators, B*, 2014, **202**, 788; (*g*) C. Patra, A. K. Bhanja, C. Sen, D. Ojha, D. Chattopadhyay, A. Mahapatra and C. Sinha, *Sens. Actuators, B*, 2016, **228**, 287; (*h*) V. Bhalla, V. Vij, M. Kumar, P. R. Sharma and T. Kaur, *Org. Lett.*, 2012, **14**, 1012.

9 C. He, W. Zhu, Y. Xu, Y. Zhong, J. Zhou and X. Qian, *J. Mater. Chem.*, 2010, **20**, 10755.

10 (*a*) J. Xu, C. Shen, X. Zhu, P. Zhang, M. J. Ajitha, K. Huang, Z. An and X. Liu, *Chem.–Asian J.*, 2016, **11**, 882; (*b*) J. Xu, X. Zhu, G. Zhou, B. Ying, P. Ye, L. Su, C. Shen and P. Zhang, *Org. Biomol. Chem.*, 2016, **14**, 3016; (*c*) B. Ying, J. Xu, X. Zhu, C. Shen and P. Zhang, *ChemCatChem*, 2016, **8**, 2604; (*d*) X. Zhu, L. Qiao, P. Ye, B. Ying, J. Xu, C. Shen and P. Zhang, *RSC Adv.*, 2016, **6**, 89979.

11 (*a*) L. Gu, X. Wan, H. Liu, T. Liu and Y. Yao, *Anal. Methods*, 2014, **6**, 8460; (*b*) Z. Liu, C. Zhang, Y. Chen, F. Qian, Y. Bai, W. He and Z. Guo, *Chem. Commun.*, 2014, **50**, 1253; (*c*) L. Xue, G. Li, C. Yu and H. Jiang, *Chem.–Eur. J.*, 2012, **18**, 1050; (*d*) Y. Ma, H. Chen, F. Wang, S. Kambam, Y. Wang, C. Mao and X. Chen, *Dyes and Pigments*, 2014, **102**, 301.

12 J. L. Palma, A. Evrim, H. Lindsay, T. B. Marder, J. C. Collings, B. Andrew, J. S. Melinger, J. L. Krause and V. D. Kleiman, *J. Phys. Chem. C*, 2010, **114**, 20702.

13 J. Hou, H. Y. Chen, S. Zhang, G. Li and Y. Yang, *J. Am. Chem. Soc.*, 2008, **130**, 16144.

14 (*a*) Y. Zhang, X. Guo, W. Si, L. Jia and X. Qian, *Org. Lett.*, 2008, **10**, 473; (*b*) S. Goswami, A. K. Das, K. Aich, A. Manna, S. Maity, K. Khanra and N. Bhattacharyya, *Analyst*, 2013, **138**, 4593.

15 (*a*) F. Qian, C. Zhang, Y. Zhang, W. He, X. Gao, P. Hu and Z. Guo, *J. Am. Chem. Soc.*, 2009, **131**, 1460; (*b*) L. Tang, X. Dai, K. Zhong, D. Wu and X. Wen, *Sens. Actuators, B*, 2014, **203**, 557; (*c*) K. Ponnuvel, M. Kumar and V. Padmini, *Sens. Actuators, B*, 2016, **227**, 242.